Supporting Information

Synthesis of ITIC Derivatives with Extended π-Conjugation as Non-Fullerene Acceptors for Organic Solar Cells

Hee Su Kim[†], Chang Eun Song[¶], Jong-Woon Ha[†], Suha Lee[†], Shafket Rasool[¶], Hang Ken Lee[¶], Won Suk Shin[¶], and Do-Hoon Hwang[,†]*

[†]Department of Chemistry and Chemistry Institute for Functional Materials, Pusan National University, Busan 46241, Republic of Korea

[¶]Energy Materials Research Center, Korea Research Institute of Chemical Technology (KRICT), Daejeon 34114, Republic of Korea

[*] E-mail address: dohoonhwang@pusan.ac.kr (D.-H. Hwang)

Tel.:+82-51-510-2232

Fax:+82-51-516-7421

EXPERIMENATL

Materials

All water and air sensitive reactions were carried out under a N2 atmosphere. The reagents and starting materials were purchased from commercial suppliers (Aldrich, TCI Korea, or ThermoFisher Scientific) and were used without further purification. Tris(dibenzylideneacetone)dipalladium (0) was purchased from Strem Chemicals. Poly[(2,6-(4,8-bis(5-(2-ethylhexyl)thiophen-2-yl)-benzo[1,2-*b*:4,5-*b*']dithiophene))-*alt*-(5,5-(1',3'-di-2-thienyl-5',7'-bis(2-ethylhexyl)benzo[1',2'-*c*:4',5'-*c*']dithiophene-4,8-dione)] (PBDB-T) 3,9-bis(2-methylene-(3-(1,1-dicyanomethylene)-indanone))-5,5,11,11-tetrakis(4-hexylphenyl)-dithieno[2,3-*d*:2',3'-*d*']-*s*-indaceno[1,2-*b*:5,6-*b*']dithiophene (ITIC) were purchased from 1-Materials. Further, 2-(5,6-difluoro-3-oxo-2,3-dihydro-1*H*-inden-1-ylidene)malononitrile (FINCN) was purchased from Derthon Optoelectronic Materials Science Technology Co., Ltd. Solvents were dried and purified by fractional distillation over sodium/benzophenone and handled in a moisture-free atmosphere. Column chromatography was performed using silica gel (Electronic Materials Index, SL-60-60A).

Characterization

^{1}H-NMR spectra were recorded using a Varian Mercury Plus 300 MHz spectrometer and ^{13}C, ^{19}F-NMR spectra were recorded using 600 MHz Agilent Superconducting FT-NMR spectrometer system. The elemental analysis was carried out using a Vario Micro Cube at the Korea Basic Science Institute (Busan, Korea). Thermogravimetric analyses were performed on a TA Instrument Q500 under a N_2 atmosphere at a heating and cooling rate of 10 °C min^{-1}. Absorption spectra were measured using a UV-1800 UV-VIS spectrophotometer. Cyclic voltammetry (CV) measurements were performed on a CH Instruments Electrochemical Analyzer. The CV measurements were performed in acetonitrile containing 0.1 M Bu_4NBF_4 as the supporting electrolyte using Ag/$AgNO_3$, a platinum wire, and platinum as the reference, counter, and working electrodes, respectively. Density functional theory (DFT) calculations to calculate the highest occupied molecular orbital (HOMO) and lowest unoccupied molecular orbital (LUMO) energies were carried out using Gaussian 09W with Becke's three-parameter functional with Lee–Yang–Parr correlation (B3LYP) and the 6-31G(d) basis set.

Photoluminescence (PL) spectra were recorded using a Hitachi JP/F-7000 spectrophotometer. Two-dimensional grazing incident X-ray diffraction (2D-GIXD) experiments were performed under vacuum at the 3C beamline of the Pohang Accelerator Laboratory (PAL) in Korea. To obtain results comparable to those of the organic solar cell (OSC) devices, the samples were prepared on zinc oxide (ZnO)-modified Si substrates under the same conditions as those used for the fabrication of solar cell devices. The wavelength of the X-rays was 1.2301 Å (10.0791 keV) and the incidence angle (the angle between the critical angle of the sample and that of Si) was 0.16°. The surface morphologies of the blend thin films were characterized using atomic force microscopy (AFM; SPM System Co., Ltd.) operated in tapping mode.

Fabrication of inverted photovoltaic devices

Patterned indium tin oxide (ITO) glass substrates were cleaned in warm detergent, deionized water, acetone, and isopropanol in an ultrasonic bath for 15 min successively, followed by UV−ozone treatment for 20 min. The zinc oxide nanoparticle (ZnO NP) solution (the particles were dispersed in n-butanol) was dropped onto the

substrates and spun at 4000 rpm for 40 s. Subsequently, the ZnO-coated glass substrates were baked at 100 °C for 10 min on a hot plate. In addition, a polyethylenimine ethoxylated (PEIE) layer was deposited onto the ZnO films using a PEIE solution at 4000 rpm for 60 s. The blended active solution, that is, PBDB-T:acceptor, dissolved in chlorobenzene (total: 13.5 mg mL^{-1}), was spin-cast onto the substrates at 2000 rpm for 30 s in a nitrogen-filled glove box. Finally, 10 nm of MoO_3 and 100 nm of Ag were thermally evaporated as the anode in the vacuum chamber at a base pressure of 3×10^{-6} Torr. The device performance was measured in air at room temperature, and the effective area of the device was 0.12 cm^2.

The SCLC method was employed to measure the hole-only and electron-only mobility of the PBDB-T/acceptor blends using a device with the following structure: ITO/PEDOT:PSS/active layer/Au (hole-only) and ITO/ZnO NPs/PEIE/active layer/Ca/Al (electron-only). The charge mobility was calculated using the following equation:

$$J_{SCLC} = (9/8)\varepsilon_r \varepsilon_0 \mu (V^2 / L^3),$$

where J is the current density, ε_r is the dielectric constant of the polymers, ε_o is the vacuum permittivity, μ is the hole mobility, L is the thickness of the blend films, and $V = V_{appl} - V_{bi}$, where V_{appl} and V_{bi} are the applied potential and built-in voltage resulting from the difference in the work functions of the anode and cathode, respectively. The photovoltaic properties were characterized under simulated AM 1.5G (100 mW/cm^2) irradiation from a xenon arc lamp. The solar simulator (Newport) intensity was set using a National Renewable Energy Laboratory (NREL)-certified silicon diode with an integrated KG5 optical filter. The current-density–voltage characteristics of the devices were measured using a computer-controlled Keithley 236 source measure unit (Keithley Instruments). The external quantum efficiency (EQE) was measured using a K3100 spectral IPCE measurement system (McScience, South Korea). All device measurements were carried out in air at room temperature.

Fabrication of inverted sub-module organic photovoltaic cells

Inverted sub-modules were fabricated in air using a D-bar coater (PEMS; printed electro mechanical system, South Korea). A 1.40-wt% donor:acceptor (1:1) solution was prepared in chlorobenzene solvent using 0.5 vol% 1,8-diiodooctane (DIO) and stirred at 50 °C overnight. ZnO NPs (bought from Nano Clean Tech, NCT) were filtered with 0.45-μm polytetrafluoroethylene (PTFE) filters, and a 30-nm layer of ZnO electron transport layer (ETL) was bar coated at a bar speed of 7-mm/s and, then, annealed at 100 °C for 10 min. The PEIE layer was deposited onto the ZnO films from the diluted PEIE solution at a bar speed of 7-mm/s and then annealed at 100 °C for 10 min. The photoactive solution was also filtered with a 0.4-μm PTFE filter, and 100 nm of the photoactive film was coated over the ZnO/PEIE layer. Them, 20 μL of the solution was dropped onto each bar, and a bar speed of 15 mm/s was used for film coating. Photoactive films were pre-annealed at 90 °C/10 min before the deposition of the top electrode. Finally, the sub-module was completed by depositing 10 nm of thermally

evaporated MoO_3 and 100 nm of Ag under a 3 × 10^{-6} Torr vacuum. The PCEs were measured using a mask of area 56.266 cm^2.

Stability testing conditions of OSCs

For ambient stability testing, the OSCs were placed into air without the encapsulation. While, glass-to-glass encapsulated devices using UV-curable epoxy-resin were placed into the light soaking (LS) weathering chamber, which is equipped with controlled temperature, humidity and light intensity. PCEs of the OSCs in both kinds of stability testing were measured under 1 Sun illumination in air.

Details of molecular acceptor syntheses

6,6,12,12-Tetrakis(4-hexylphenyl)-6,12-dihydro-dithieno[2,3-d:2',3'-d]-s-indaceno[1,2-b:5,6-b']dithiophene-2-carboxaldehyde (1): To a solution of 6,6,12,12-tetrakis(4-hexylphenyl)-6,12-dihydro-dithieno[2,3-*d*:2′,3′-*d*′]-*s*-indaceno[1,2-*b*:5,6-*b*′]dithiophene (3 g, 2.94 mmol) in 1,2-dichloroethane (DCE, 30 mL) at 0 °C, dimethylformamide (DMF, 0.68 mL, 3 equiv), and phosphorus (V) oxychloride ($POCl_3$,

0.41 mL, 1.5 equiv) was added dropwise sequentially under nitrogen (N_2) atmosphere. The mixture was then stirred 12 h at room temperature and quenched with sodium acetate solution. The mixture was extracted with dichloromethane three times. After drying over $MgSO_4$, the solvent was removed and purified with column chromatography using dichloromethane:hexane (1:1) as an eluent to obtain a yellow solid. Yield: 75% (2.3 g) ^{1}H NMR (300 MHz, $CDCl_3$, ppm): δ 9.87 (s, 1H), 7.93 (s, 1H), 7.56 (s, 1H), 7.53 (s, 1H), 7.29 (m, 2H), 7.18–7.07 (m, 16H), 2.54 (t, 8H), 1.57 (m, 8H), 1.28 (m, 24H), 0.85 (t, 12H). Elemental analysis calcd for $C_{69}H_{74}OS_4$: C, 79.1; H, 7.1; S, 12.2. Found: C, 79.0; H, 7.2; S, 12.3.

8-Bromo-6,6,12,12-tetrakis(4-hexylphenyl)-6,12-dihydro-dithieno[2,3-d:2',3'-d]-s-indaceno [1,2-b:5,6-b']dithiophene-2-carboxaldehyde (2): Compound 1 (2.3 g, 2.19 mmol) was dissolved in 30 mL of chloroform, and the reaction flask was covered with aluminum foil. N-Bromosuccinimide (0.6 g, 1.5 equiv) was added to the flask at 0 °C, and the mixture was stirred at room temperature overnight and then quenched with distilled water. The mixture was extracted with chloroform twice and dried over $MgSO_4$.

The crude product obtained after the evaporation of the solvent was recrystallized from dichloromethane/ethanol to obtain a yellow solid. Yield: 93% (2.3 g). ^{1}H NMR (300 MHz, $CDCl_3$, ppm): δ 9.87 (s, 1H), 7.92 (s, 1H), 7.55 (s, 1H), 7.52 (s, 1H), 7.28 (s, 1H), 7.18–7.07 (m, 16H), 2.54 (t, 8H), 1.56 (m, 8H), 1.28 (m, 24H), 0.85 (m, 12H). Elemental analysis calcd for $C_{69}H_{73}BrOS_4$: C, 73.5; H, 6.5; S, 11.4. Found: C, 73.6; H, 6.5; S, 11.4.

FDTBT-IDTT-CHO (3): Compound 2 (1.2 g, 1.33 mmol) and 5,6-difluoro-4,7-bis(5-(trimethylstannyl)thiophen-2-yl)benzo[*c*][1,2,5]thiadiazole (FDTBT-tin, 0.30 g, 0.58 mmol, 1 equiv) were dissolved in anhydrous toluene (30 mL) under N_2. Tris(dibenzylideneacetone)dipalladium ($Pd_2(dba)_3$, 50 mg, 0.12 equiv) and tri(o-tolyl)phosphine ($P(o\text{-}tolyl)_3$, 50 mg, 0.36 equiv) were added into the flask and the mixture was stirred at 110 °C overnight. The mixture was extracted with chloroform several times and dried over $MgSO_4$. The solvent was removed and purified by silica gel column chromatography using dichloromethane:hexane (1:1) as an eluent to obtain a dark solid. Yield: 72% (0.8 g). ^{1}H NMR (300 MHz, $CDCl_3$, ppm): δ 9.87 (s,

2H), 8.21 (d,2H), 7.92 (s, 2H), 7.55 (m, 6H), 7.30 (d, 2H), 7.22–7.11 (m, 32H), 2.55 (m, 16H), 1.56 (m, 16H), 1.28 (m, 48H), 0.86 (m, 24H). Elemental analysis calcd for $C_{152}H_{150}F_2N_2O_2S_{11}$: C, 75.2; H, 6.2; N, 1.1; S, 14.5. Found: C, 75.2; H, 6.3; N, 1.2; S, 14.5.

CNDTBT-IDTT-CHO (4): Compound 2 (1.1 g, 0.97 mmol) and 4,7-bis(5-(trimethylstannyl)thiophen-2-yl)benzo[*c*][1,2,5]thiadiazole-5,6-dicarbonitrile (CNDTBT-tin, 0.30 g, 0.42 mmol, 1 equiv) was dissolved in anhydrous toluene (30 mL) under N_2. $Pd_2(dba)_3$ (50 mg, 0.12 equiv) and P(o-tolyl)$_3$ (50 mg, 0.36 equiv) were added to the flask and the mixture was stirred at 110 °C overnight. The mixture was extracted with chloroform several times and dried over $MgSO_4$. The solvent was removed and purified by silica gel column chromatography using dichloromethane:hexane (1:1) as an eluent to obtain a dark solid. Yield: 83% (0.9 g). ^{1}H NMR (300 MHz, $CDCl_3$, ppm): δ 9.87 (s, 2H), 8.27 (d,2H), 7.93 (s, 2H), 7.60 (m, 6H), 7.33 (d, 2H), 7.22–7.11 (m, 32H), 2.55 (m, 16H), 1.56 (m, 16H), 1.28 (m, 48H),

0.86 (m, 24H). Elemental analysis calcd for $C_{154}H_{150}N_4O_2S_{11}$: C, 75.7; H, 6.2; N, 2.3; S, 14.4. Found: C, 75.8; H, 6.2; N, 2.3; S, 14.6.

FDTBT-IDTT-FINCN (5): Compound 3 (0.30 g, 0.12 mmol) and 2-(5,6-difluoro-3-oxo-2,3-dihydro-1H-inden-1-ylidene)malononitrile (FINCN, 0.2 g, 7 equiv) were dissolved in anhydrous chloroform (30 mL) under N_2. Subsequently, pyridine (0.2 mL) was added dropwise, and the mixture was stirred overnight at 65 °C. The mixture was allowed to cool to room temperature and added slowly into 100 mL of methanol with vigorous stirring. The crude product was collected by filtration and purified by silica gel column chromatography using dichloromethane:hexane (1:1) as the eluent to obtain a dark solid. Yield: 85% (0.33 g). ^{1}H NMR (300 MHz, $CDCl_3$, ppm): δ 8.82 (s, 2H), 8.54 (m, 2H), 8.20 (m, 4H), 7.67 (m, 4H), 7.54 (m, 4H), 7.28–7.14 (m, 32H), 2.57 (m, 16H), 1.60 (m, 16H), 1.29 (m, 48H), 0.86 (m, 24H). ^{13}C NMR (150 MHz, $CDCl_3$, ppm): δ 185.61, 158.28, 155.73, 155.15, 154.91, 154.11, 153.52, 148.63, 148.18, 147.79, 146.67, 143.43, 143.09, 142.31, 142.11, 140.99, 139.50, 139.06, 138.87, 138.75, 138.71, 138.31, 137.36, 136.54, 134.51, 133.17, 131.93, 130.95, 128.73, 128.59,

127.90, 127.84, 124.11, 121.16, 118.44, 117.30, 117.06, 114.74, 114.28, 114.17, 112.51, 111.29, 69.24, 63.16, 62.99, 35.51, 31.60, 31.10, 29.06, 22.17, 13.91. ^{19}F NMR (564 MHz, $CDCl_3$, ppm): δ -122.91 (m), -124.08 (m), -127.77 (s). Elemental analysis calcd for $C_{176}H_{154}F_6N_6O_2S_{11}$: C, 74.1; H, 5.4; N, 2.9; S, 12.4. Found: C, 74.1; H, 5.5; N, 3.0; S, 12.4. MS (matrix-assisted laser desorption/ionization (MALDI)-time of flight (TOF) mass spectrometry) m/z: 2848.90 [M^+], calcd 2849.43.

CNDTBT-IDTT-FINCN (6): Compound 4 (0.30 g, 0.12 mmol) and 2-(5,6-difluoro-3-oxo-2,3-dihydro-1H-inden-1-ylidene)malononitrile (FINCN, 0.2 g, 7 equiv) was dissolved in anhydrous chloroform (30 mL) under N_2. Subsequently, pyridine (0.2 mL) was added dropwise, and the mixture was stirred overnight at 65 °C. The mixture was allowed to cool to room temperature and added slowly into 100 mL of methanol with vigorous stirring. The crude product was collected by filtration and purified by silica gel column chromatography using dichloromethane:hexane (1:1) as the eluent to obtain a dark solid. Yield: 86% (0.34 g). ^{1}H NMR (300 MHz, $CDCl_3$, ppm): δ 8.83 (s, 2H), 8.54 (m, 2H), 8.27 (d, 2H), 8.20 (s, 2H), 7.68 (m, 4H), 7.56 (s, 2H), 7.32 (d, 2H), 7.25–7.15

(m, 32H), 2.60 (m, 16H), 1.60 (m, 16H), 1.30 (m, 48H), 0.86 (m, 24H). ^{13}C NMR (150 MHz, $CDCl_3$, ppm): δ 185.74, 158.29, 155.69, 154.81, 154.13, 153.50, 152.91, 148.15, 147.57, 146.70, 144.97, 143.91, 143.41, 142.37, 142.22, 139.42, 139.04, 138.91, 138.53, 138.38, 137.73, 137.56, 136.58, 134.76, 134.43, 133.84, 133.60, 132.03, 131.32, 128.77, 128.66, 127.84, 127.84, 124.24, 121.13, 118.49, 118.34, 117.23, 116.57, 114.32, 114.20, 112.58, 109.72, 69.26, 63.12, 62.96, 35.55, 31.64, 31.21, 29.13, 29.11, 22.53, 14.02. ^{19}F NMR (564 MHz, $CDCl_3$, ppm): δ -122.82 (m), -124.00 (m). Elemental analysis calcd for $C_{178}H_{154}F_4N_8O_2S_{11}$: C, 74.6; H, 5.4; N, 3.9; S, 12.3. Found: C, 74.6; H, 5.5; N, 3.9; S, 12.4. MS (MALDI-TOF) m/z: 2862.91 [M^+], calcd 2863.23.

1. TGA curves for the acceptors

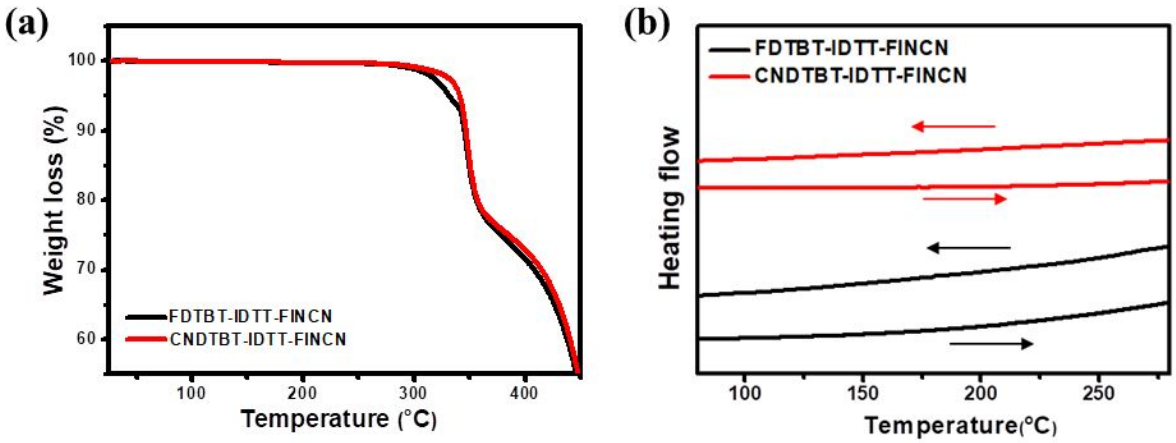

Figure S1. (a) Thermogravimetric analysis curves and (b) DSC thermograms of the synthesized acceptors.

2. Absorption coefficients of the acceptors

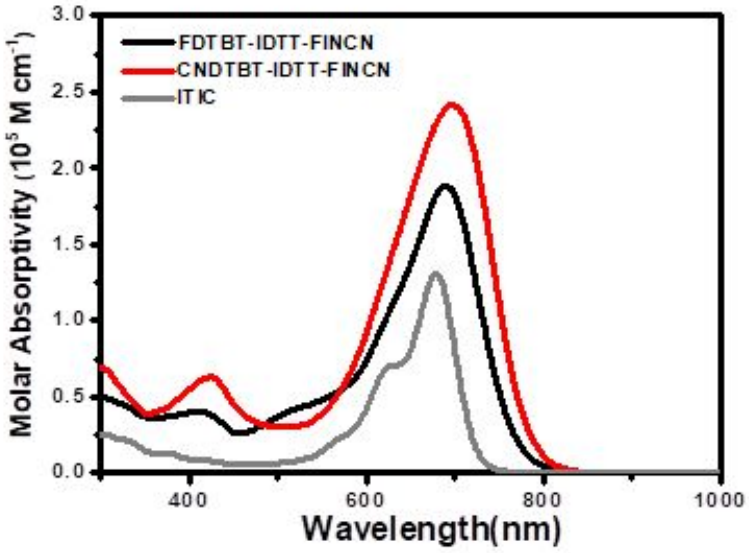

Figure S2. Molar absorptivity of the molecular acceptors in chloroform.

3. DFT calculated HOMOs and LUMOs

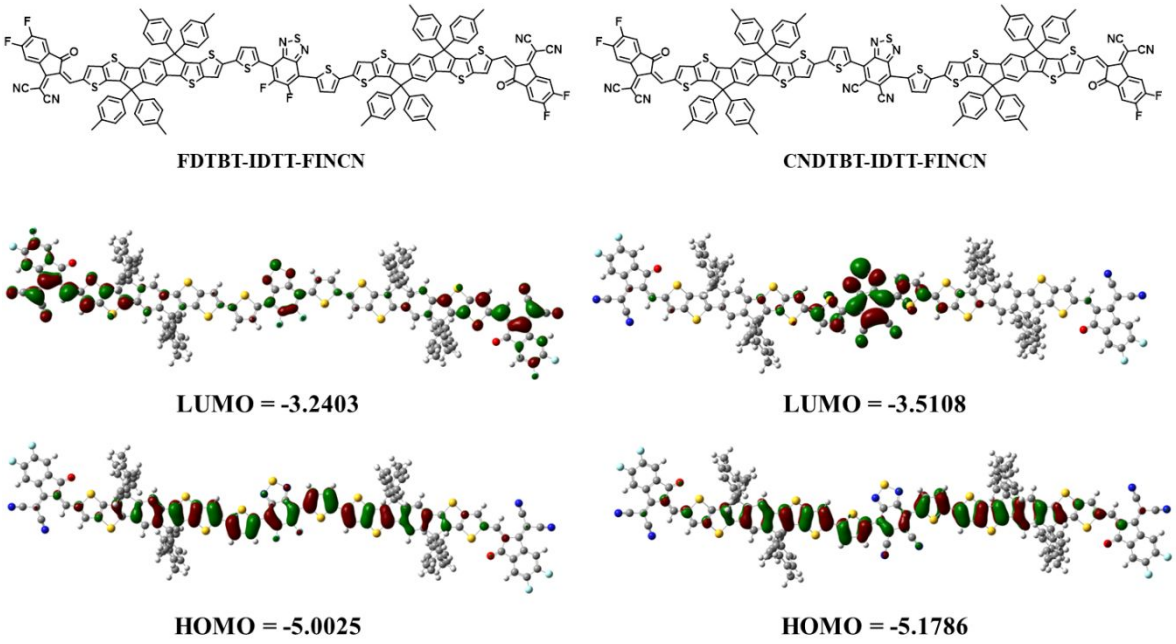

Figure S3. Energy-minimized structure (B3LYP/6-31G (d)) of the HOMOs and LUMOs of the model compounds at the bottom and top, respectively. The yellow, red, and blue symbols represent sulfur, oxygen, and nitrogen atoms, respectively.

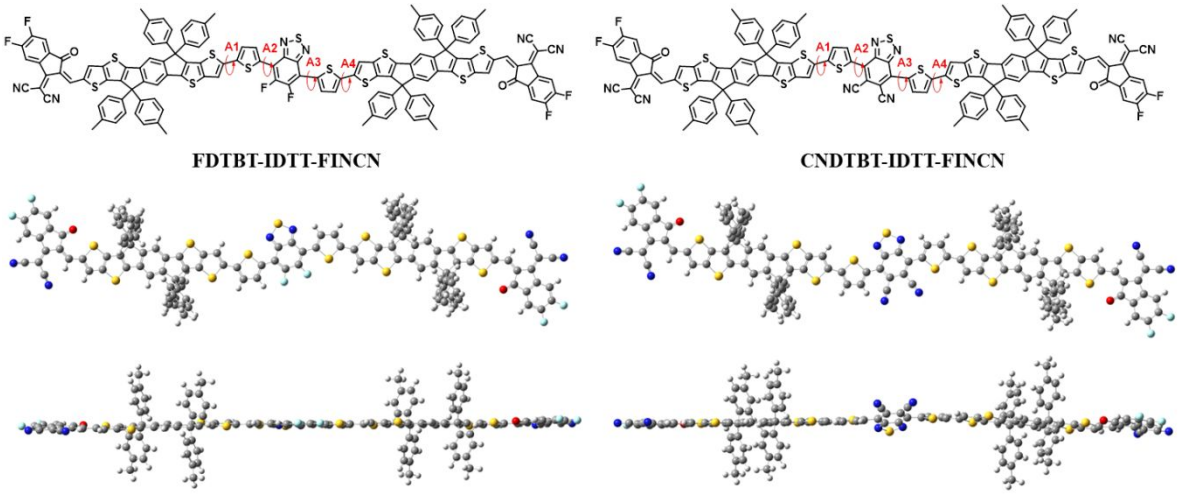

Figure S4. Dihedral angles of the minimum energy geometries of the model compounds and their side and top views calculated using DFT at the B3LYP/6-31G (d) level of theory.

Table S1. Dihedral angles of the model compounds calculated by DFT.

Acceptor	Dihedral angle (°)			
	A_1	A_2	A_3	A_4
FDTBT-IDTT-FINCN	9.42	0.25	0.26	2.49
CNDTBT-IDTT-FINCN	3.83	24.68	16.94	26.77

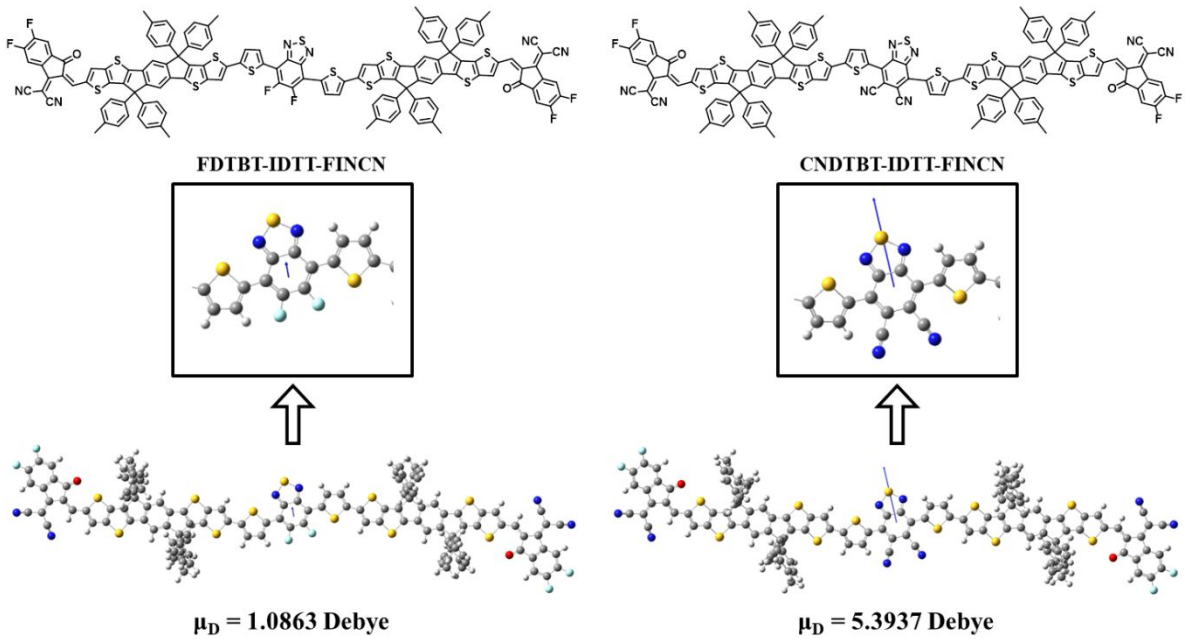

Figure S5. DFT calculated (B3LYP/6-31G (d)) dipole moments of the acceptors.

4. Organic photovoltaic (OPV) device optimization

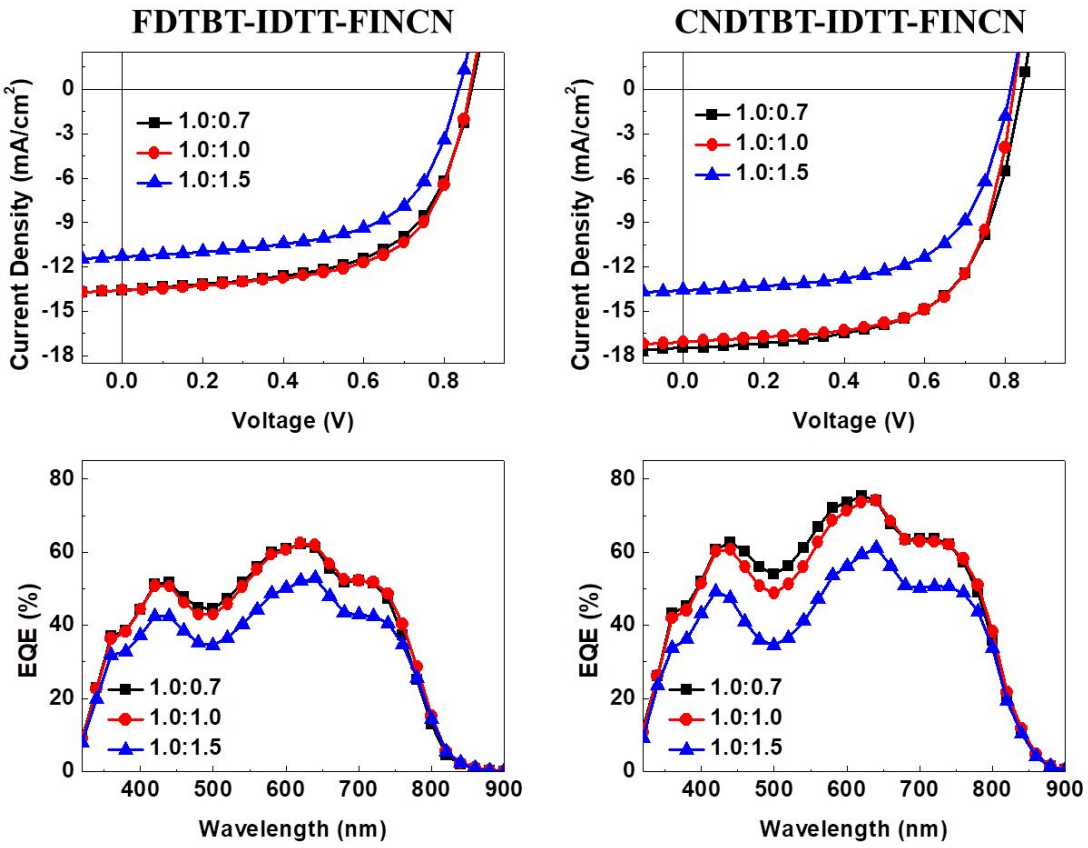

Figure S6. *J-V* and *EQE* curves of PBDB:T:acceptor bulk heterojunction (BHJ) OPVs having different D:A blend ratios.

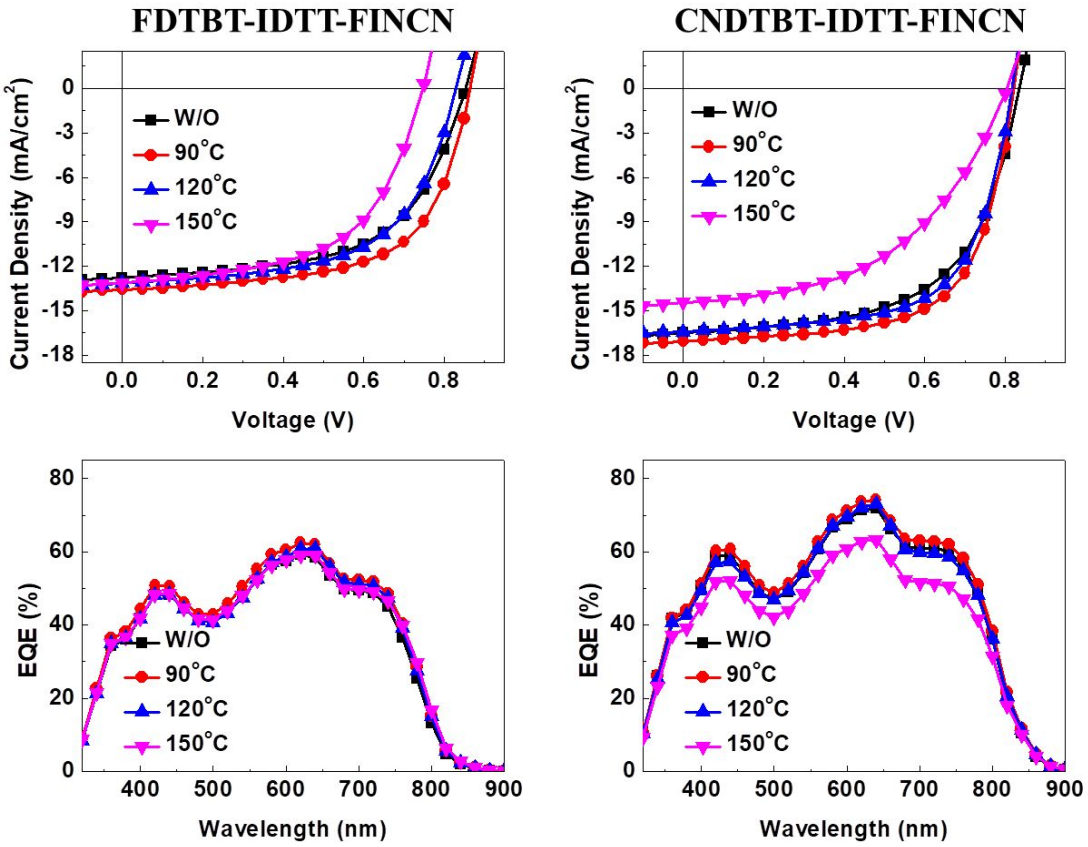

Figure S7. *J-V* and *EQE* curves of PBDB:T:acceptor BHJ OPVs PSCs with thermal annealing.

Table S2. Summary of device parameters of the inverted OPVs based on PBDB-T:FDTBT-IDTT-FINCN.

Acceptor	Weight Ratio	Annealing	V_{OC} [V]	J_{SC} [mA/cm^2]	*FF* [%]	PCE [%]
FDTBT-IDTT-FINCN	1.0:0.7	W/O	0.87 (0.87±0.01)[a)]	12.83 (12.48±0.36)[a)]	54 (51±2)[a)]	6.01 (5.68±0.34)[a)]
		90°C, 10min	0.87 (0.85±0.02)[a)]	13.56 (13.19±0.37)[a)]	60 (60±1)[a)]	7.04 (6.72±0.32)[a)]
		130°C, 10min	0.82 (0.82±0.01)[a)]	13.61 (13.24±0.35)[a)]	60 (59±2)[a)]	6.75 (6.48±0.29)[a)]
		170°C, 10min	0.73 (0.73±0.01)[a)]	13.18 (12.96±0.21)[a)]	54 (53±1)[a)]	5.26 (4.90±0.35)[a)]
	1.0:1.0	W/O	0.85 (0.85±0.01)[a)]	12.79 (12.41±0.37)[a)]	58 (57±1)[a)]	6.33 (6.05±0.27)[a)]
		90°C, 10min	0.86 (0.85±0.01)[a)]	13.57 (13.18±0.39)[a)]	62 (61±1)[a)]	7.27 (7.08±0.20)[a)]
		130°C, 10min	0.83 (0.82±0.01)[a)]	13.14 (12.88±0.29)[a)]	59 (59±1)[a)]	6.42 (6.20±0.23)[a)]
		170°C, 10min	0.75 (0.74±0.01)[a)]	13.11 (12.79±0.31)[a)]	56 (55±1)[a)]	5.53 (5.20±0.34)[a)]
	1.0:1.5	W/O	0.88 (0.87±0.01)[a)]	10.37 (10.08±0.30)[a)]	57 (55±2)[a)]	5.19 (4.82±0.37)[a)]
		90°C, 10min	0.87 (0.86±0.01)[a)]	10.67 (10.38±0.28)[a)]	59 (58±2)[a)]	5.48 (5.18±0.30)[a)]
		130°C, 10min	0.84 (0.84±0.01)[a)]	11.30 (10.98±0.33)[a)]	61 (60±1)[a)]	5.72 (5.39±0.33)[a)]
		170°C, 10min	0.79 (0.78±0.01)[a)]	11.12 (10.75±0.36)[a)]	58 (57±1)[a)]	5.11 (4.88±0.23)[a)]

[a)]The values in parentheses are average photovoltaic properties obtained from over 5 devices.

Table S3. Summary of device parameters of the inverted OPVs based on PBDB-T:CNDTBT-IDTT-FINCN.

Acceptor	Weight Ratio	Annealing	V_{OC} [V]	J_{SC} [mA/cm^2]	*FF* [%]	PCE [%]
CNDTBT-IDTT-FINCN	1.0:0.7	W/O	0.85 (0.85±0.01)[a)]	16.92 (16.60±0.32)[a)]	57 (57±1)[a)]	8.24 (7.92±0.32)[a)]
		90°C, 10min	0.84 (0.83±0.01)[a)]	17.45 (17.19±0.27)[a)]	62 (61±1)[a)]	9.08 (8.73±0.36)[a)]
		130°C, 10min	0.82 (0.81±0.01)[a)]	17.23 (16.87±0.36)[a)]	61 (60±1)[a)]	8.71 (8.39±0.31)[a)]
		170°C, 10min	0.77 (0.77±0.01)[a)]	16.49 (16.16±0.32)[a)]	53 (51±2)[a)]	6.77 (6.40±0.38)[a)]
	1.0:1.0	W/O	0.84 (0.83±0.01)[a)]	16.50 (16.27±0.24)[a)]	59 (57±2)[a)]	8.17 (7.88±0.29)[a)]
		90°C, 10min	0.82 (0.81±0.01)[a)]	17.06 (16.69±0.35)[a)]	65 (64±1)[a)]	9.13 (9.01±0.13)[a)]
		130°C, 10min	0.82 (0.81±0.01)[a)]	16.41 (16.07±0.34)[a)]	64 (63±1)[a)]	8.61 (8.40±0.22)[a)]
		170°C, 10min	0.80 (0.80±0.01)[a)]	14.45 (14.12±0.32)[a)]	49 (47±2)[a)]	5.68 (5.38±0.30)[a)]
	1.0:1.5	W/O	0.83 (0.83±0.01)[a)]	13.38 (13.07±0.30)[a)]	51 (50±1)[a)]	5.71 (5.39±0.32)[a)]
		90°C, 10min	0.82 (0.82±0.01)[a)]	13.68 (13.39±0.28)[a)]	59 (57±2)[a)]	6.54 (5.23±0.30)[a)]
		130°C, 10min	0.81 (0.81±0.01)[a)]	13.57 (13.26±0.31)[a)]	62 (61±1)[a)]	6.79 (6.47±0.31)[a)]
		170°C, 10min	0.79 (0.79±0.02)[a)]	13.45 (16.18±0.36)[a)]	60 (59±1)[a)]	6.39 (6.12±0.29)[a)]

[a)]The values in parentheses are average photovoltaic properties obtained from over 5 devices.

5. PL spectra of the thin films

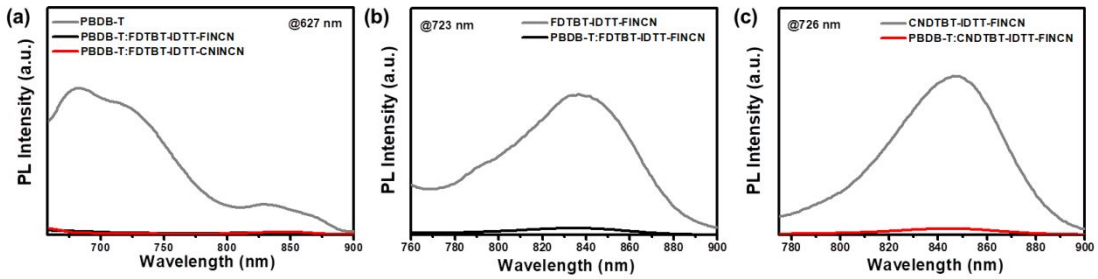

Figure S8. PL spectra of neat films and blend thin films at different excitation wavelengths for (a) PBDB-T (627 nm), (b) FDTBT-IDTT-FINCN (723 nm), and (c) CNDTBT-IDTT-FINCN (726 nm).

6. Thin-film microstructural analyses

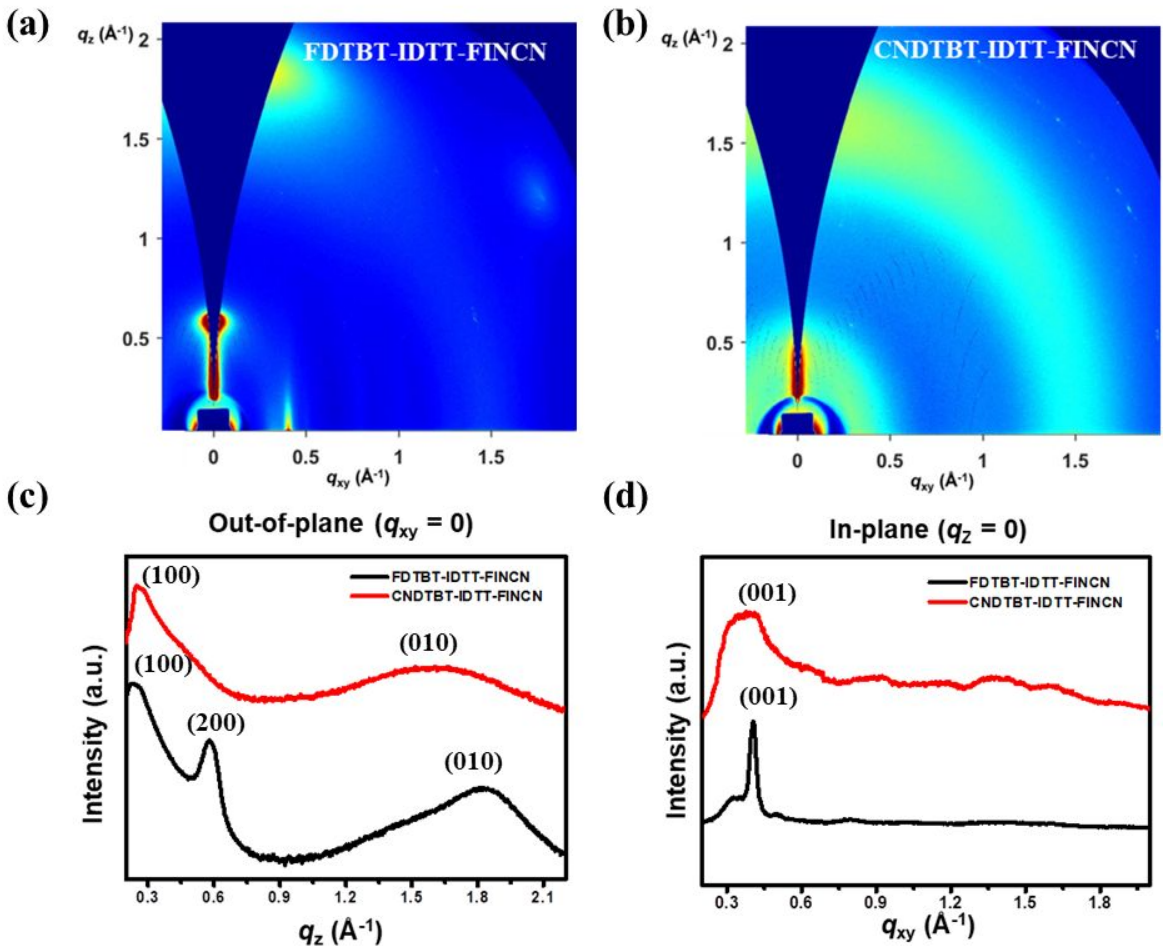

Figure S9. Two-dimensional grazing-incidence X-ray diffraction (2D-GIXD) images of the (a) FDTBT-IDTT-FINCN and (b) CNDTBT-IDTT-FINCN neat films and (c) out-of-plane and (d) in-plane XRD diffractograms.

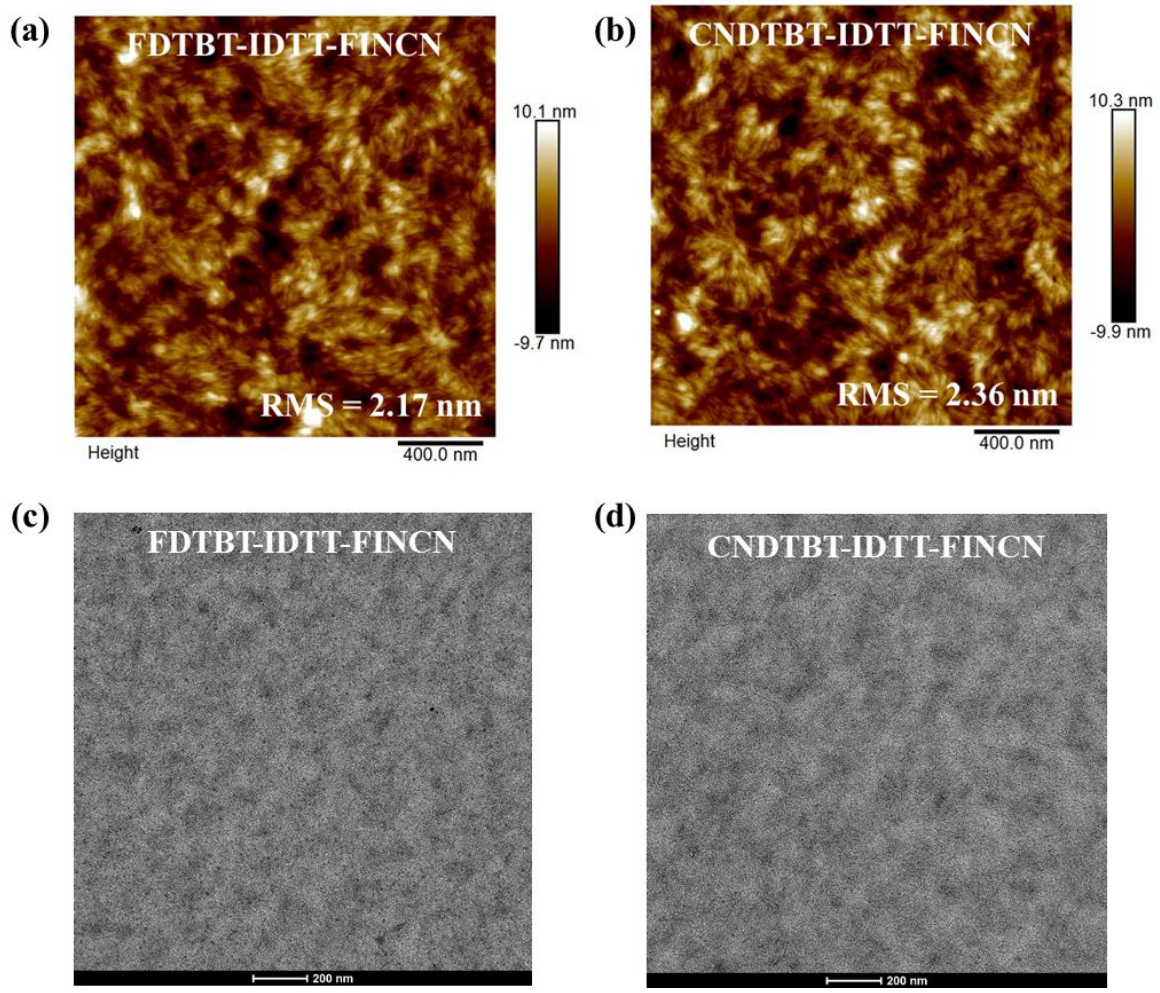

Figure S10. Surface morphology of the optimized blend films. AFM height and TEM images of (a,c) PBDB-T:FDTBT-IDTT-FINCN and (b,d) PBDB-T:CNDTBT-IDTT-FINCN.

7. Certificate of the large-area OPV device

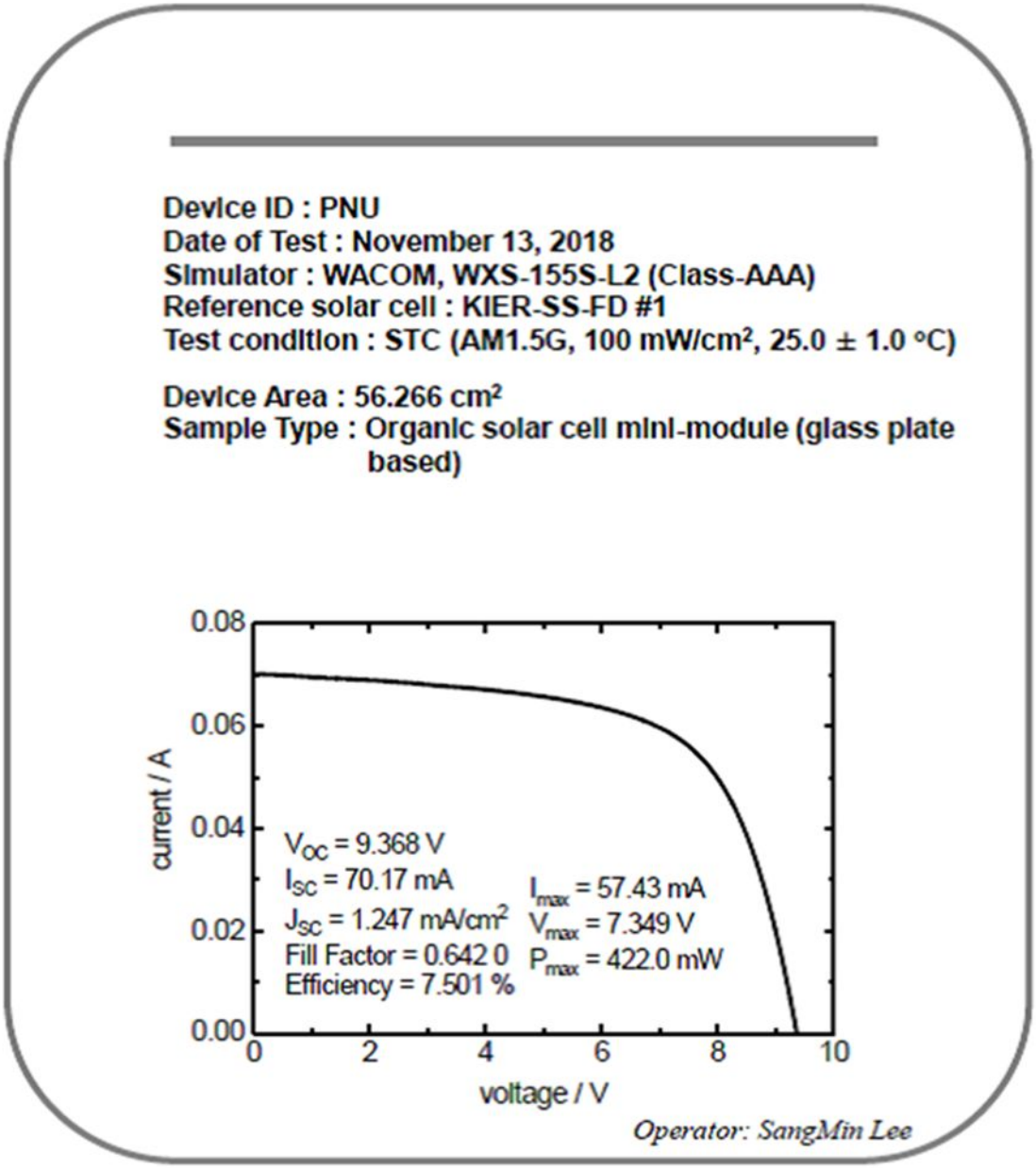

Figure S11. Certificate of 7.50% PCE for PBDB-T:CNDTBT-IDTT-FINCN for the large-area cell from the Korea Institute of Energy Research (KIER).

8. The stability of OSC devices

Table S4. The ambient and light soaking stability of OSCs based on FDTBT-IDTT-FINCN and CNDTBT-IDTT-FINCN blended with PBDB-T.

Acceptor	Condition	Ageing Time (h)										
		0h	1h	5h	20h	50h	100h	150h	200h	300h	350h	500h
FDTBT-IDTT-FINCN	Ambient	1	0.94	0.93	0.91	0.89	0.87	0.86	0.83	0.82	-	0.80
	Light soaking	1	0.93	0.89	0.79	0.75	0.74	-	0.70	-	0.67	0.60
CNDTBT-IDTT-FINCN	Ambient	1	0.96	0.95	0.93	0.90	0.88	0.87	0.85	0.84	-	0.83
	Light soaking	1	0.96	0.93	0.87	0.86	0.83	-	0.77	-	0.74	0.68

9. NMR spectrum of synthesized monomers

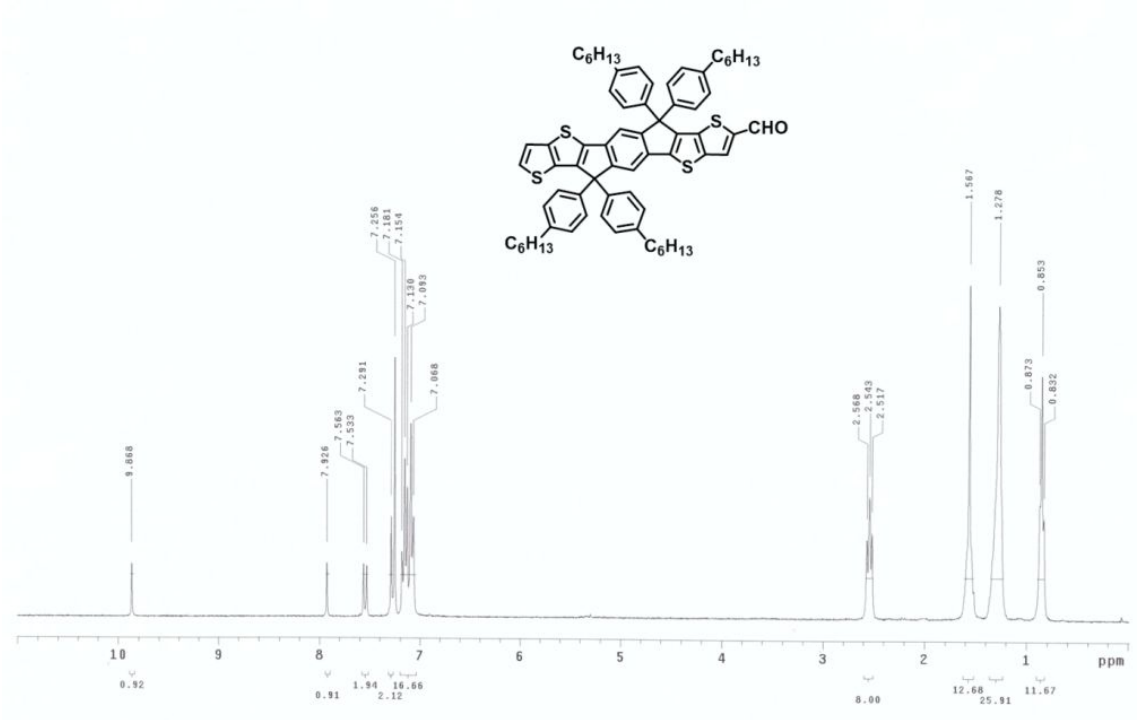

Figure S12. ^{1}H NMR spectrum of 6,6,12,12-tetrakis(4-hexylphenyl)-6,12-dihydro-dithieno[2,3-*d*:2',3'-*d*]-*s*-indaceno[1,2-*b*:5,6-*b*']dithiophene-2-carboxaldehyde.

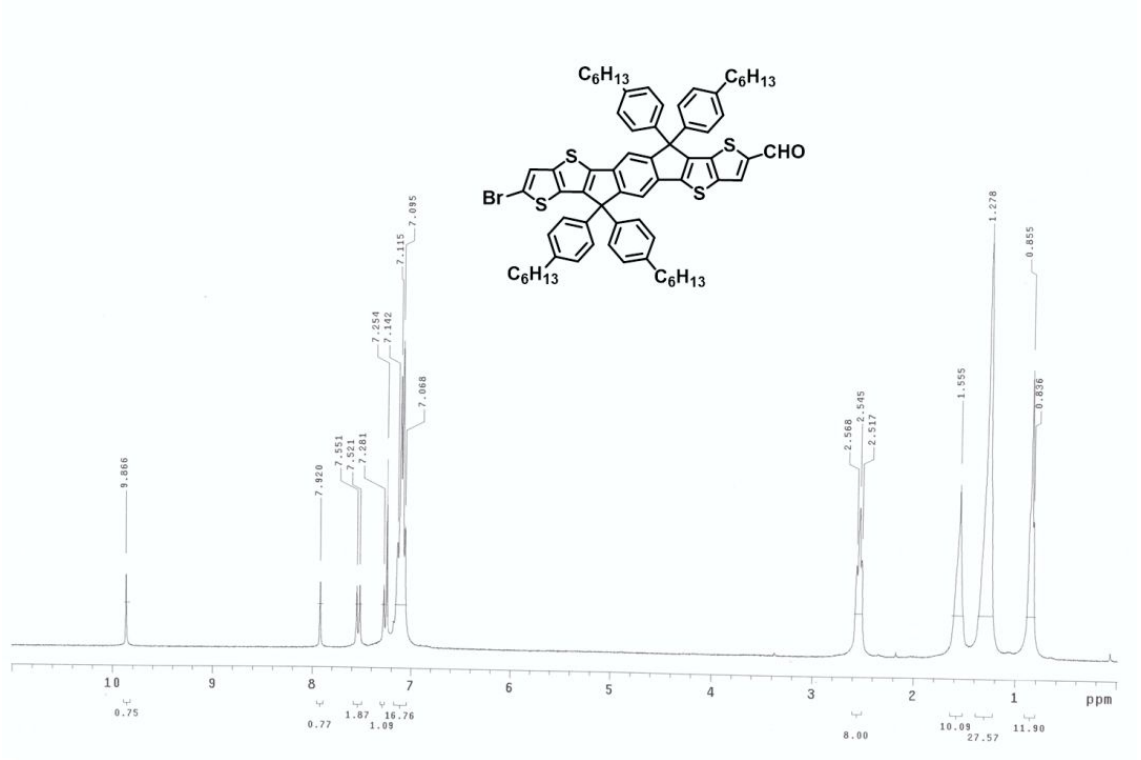

Figure S13. ^{1}H NMR spectrum of 8-bromo-6,6,12,12-tetrakis(4-hexylphenyl)-6,12-dihydro-dithieno[2,3-*d*:2',3'-*d*]-*s*-indaceno [1,2-*b*:5,6-*b*']dithiophene-2-carboxaldehyde.

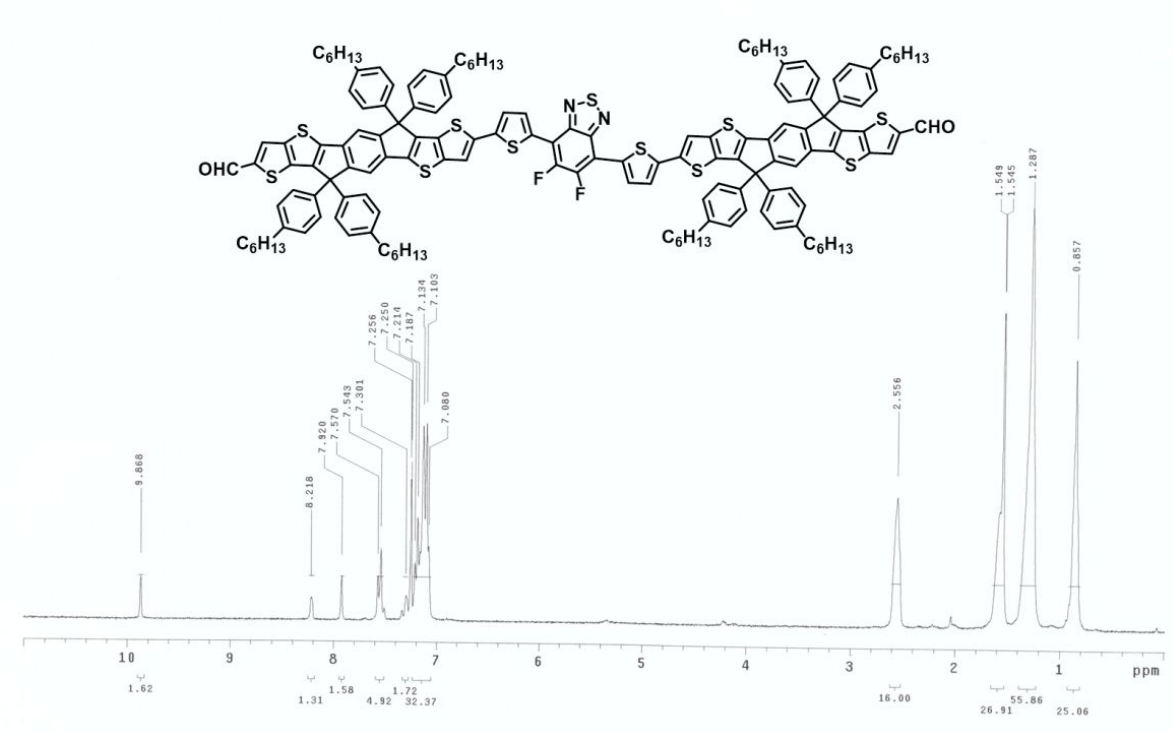

Figure S14. ^{1}H NMR spectrum of FDTBT-IDTT-CHO.

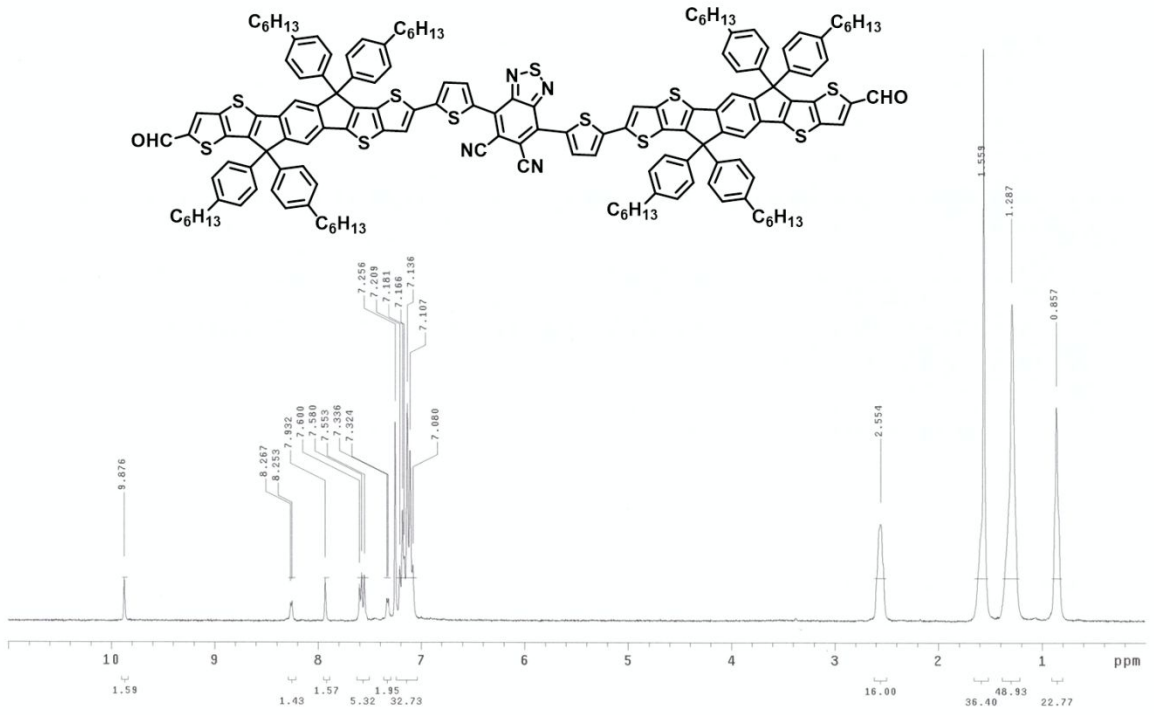

Figure S15. ^{1}H NMR spectrum of CNDTBT-IDTT-CHO.

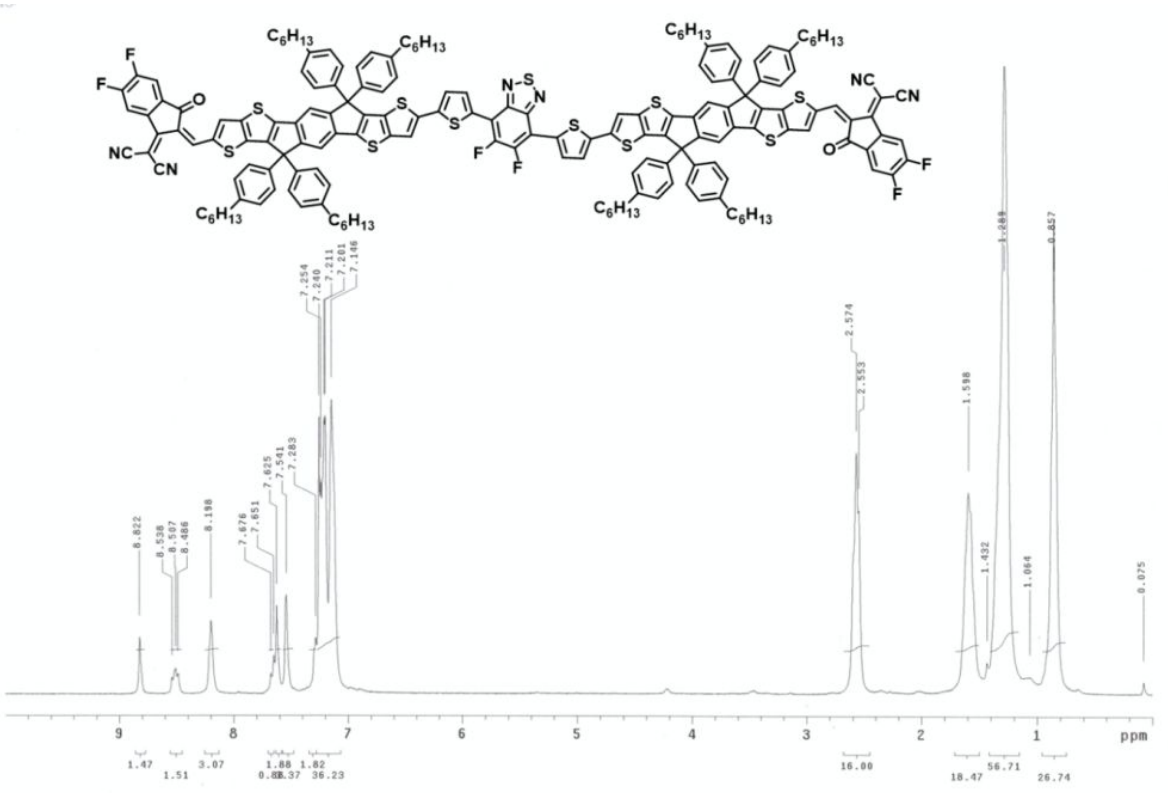

Figure S16. ^{1}H NMR spectrum of FDTBT-IDTT-FINCN.

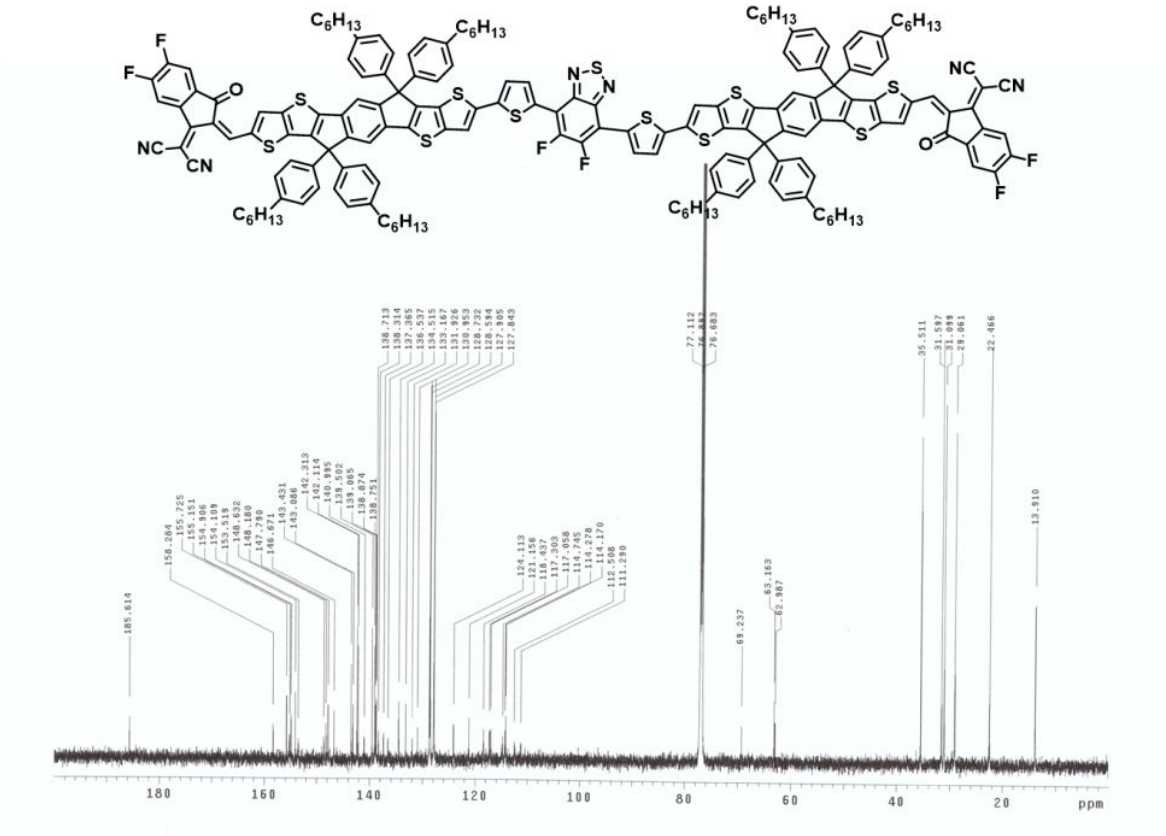

Figure S17. ^{13}C NMR spectrum of FDTBT-IDTT-FINCN.

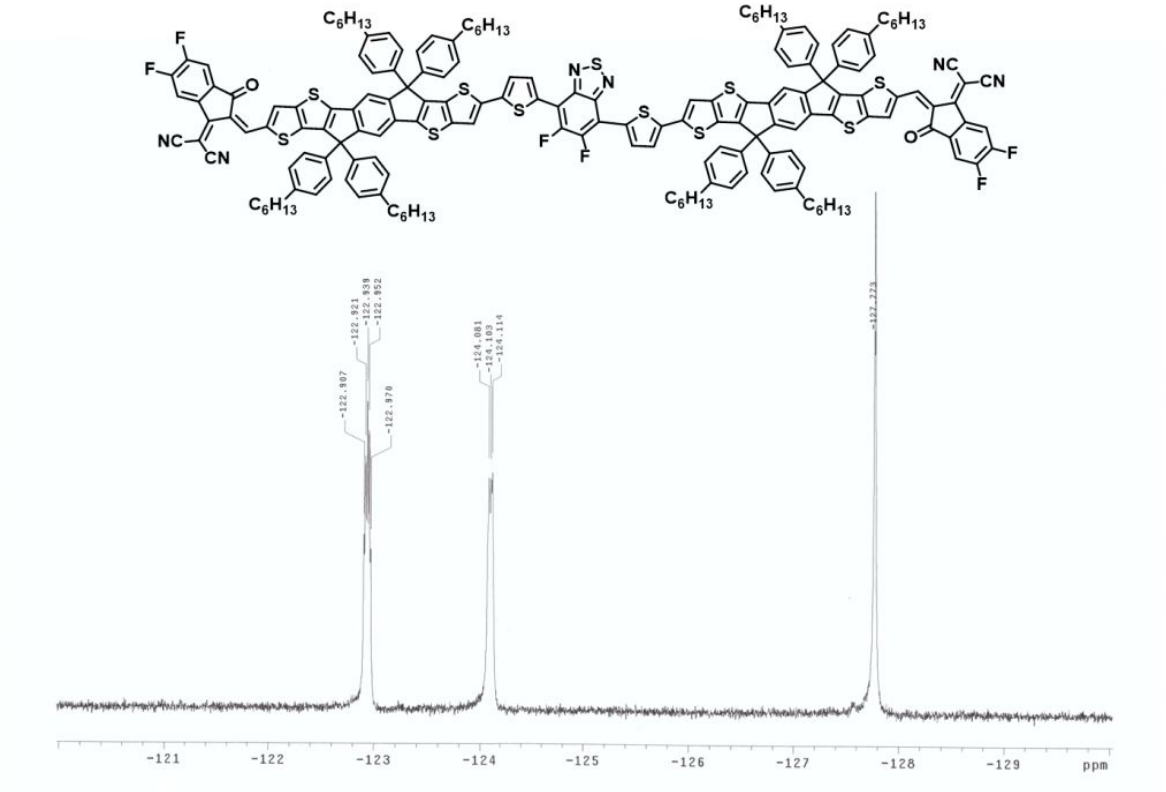

Figure S18. ^{19}F NMR spectrum of FDTBT-IDTT-FINCN.

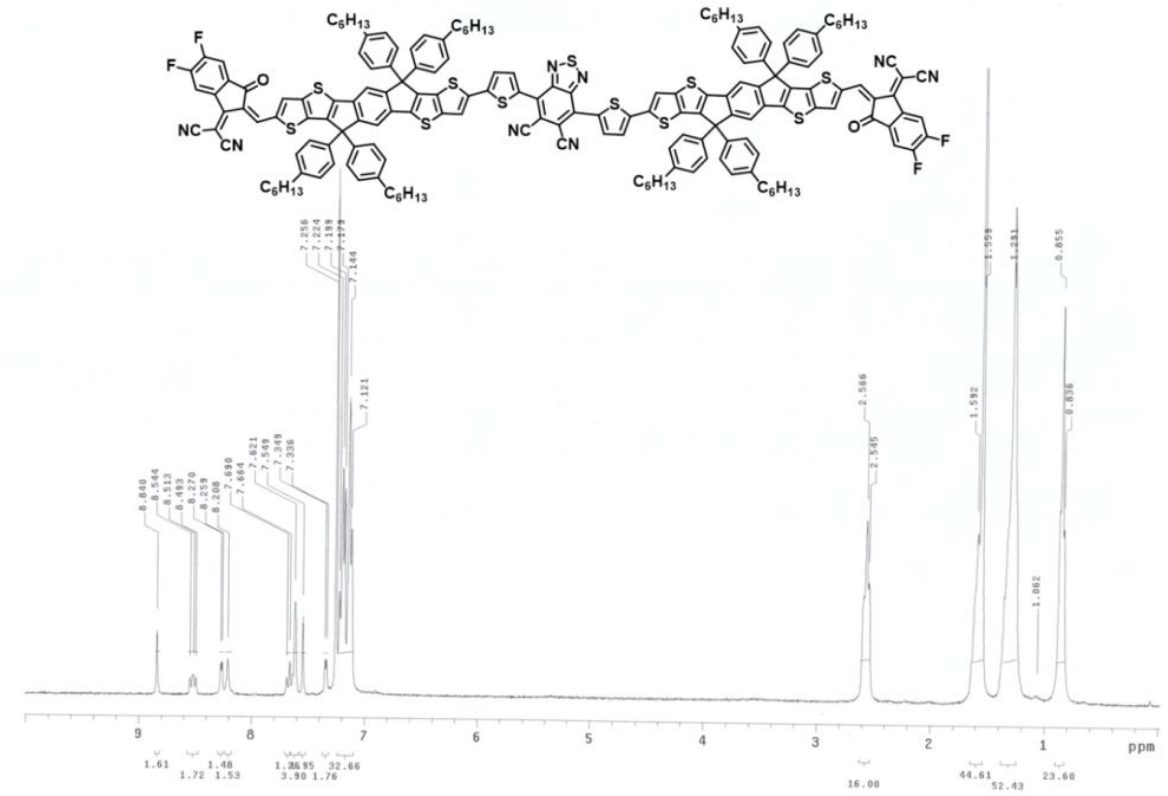

Figure S19. ^{1}H NMR spectrum of CNDTBT-IDTT-FINCN.

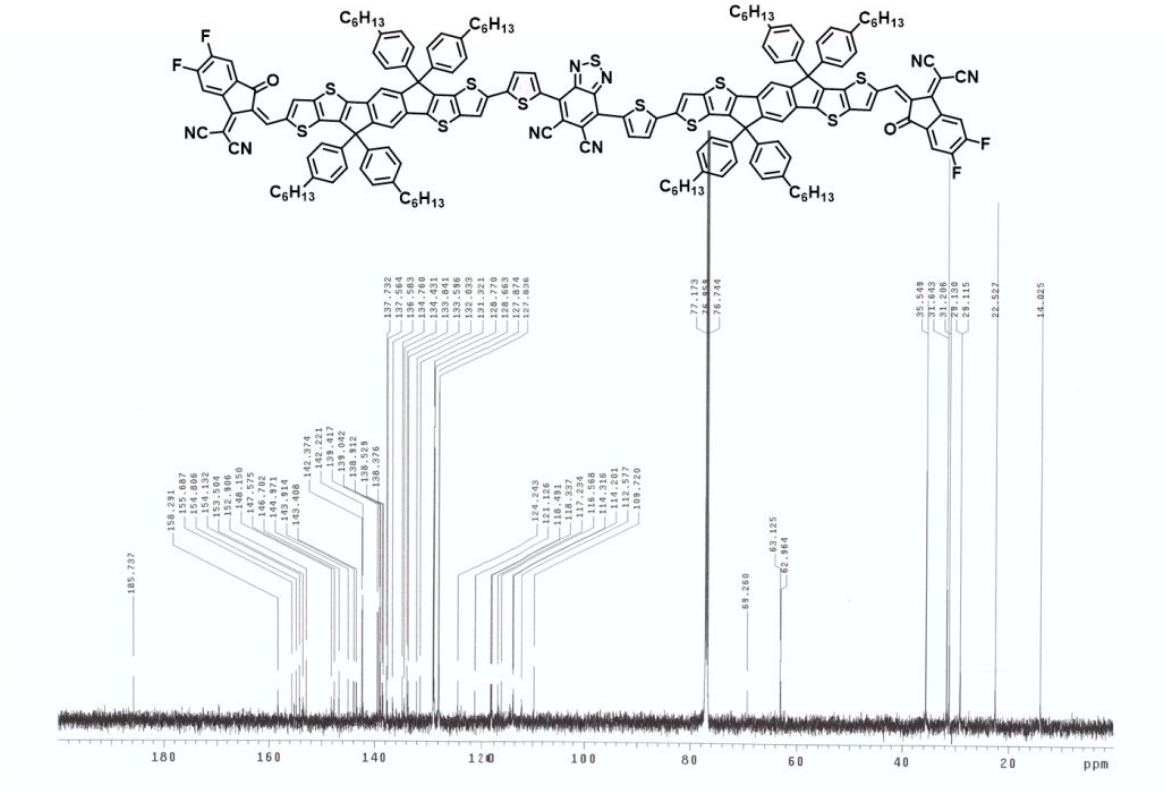

Figure S20. ^{13}C NMR spectrum of CNDTBT-IDTT-FINCN.

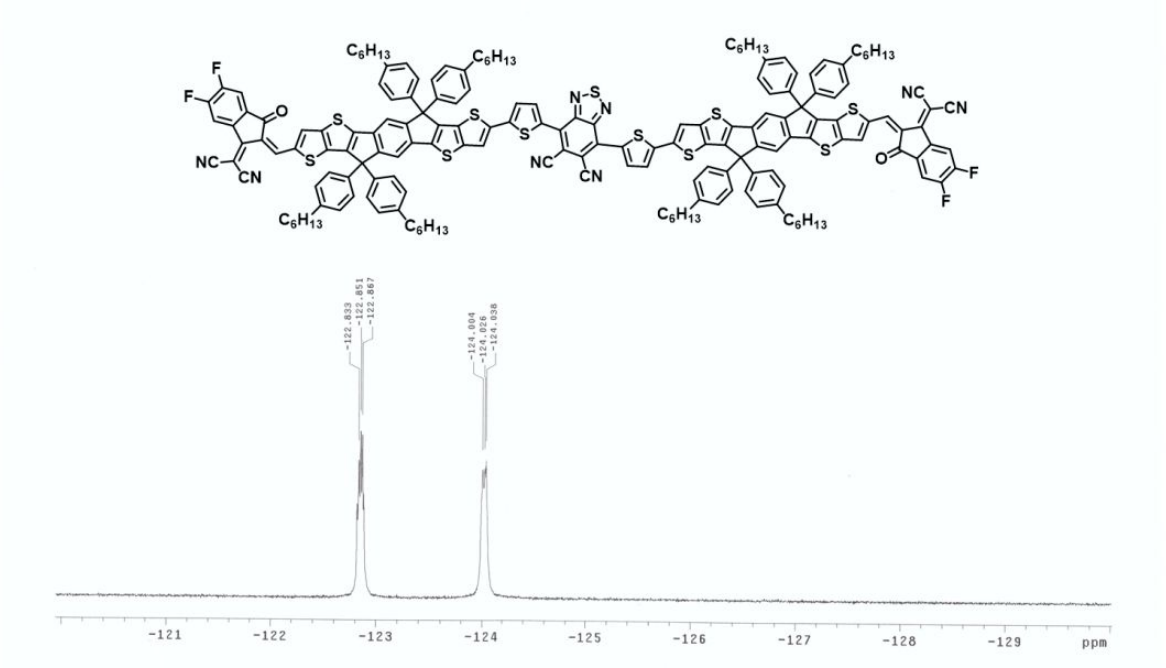

Figure S21. ^{19}F NMR spectrum of CNDTBT-IDTT-FINCN.